Available online at www.sciencedirect.com
ScienceDirect
Applied Catalysis B: Environmental 80 (2008) 248–259
APPLIED CATALYSIS B: ENVIRONMENTAL
www.elsevier.com/locate/apcatb

Study of the reaction of NO_x and soot on Fe_2O_3 catalyst in excess of O_2

D. Reichert, H. Bockhorn, S. Kureti *

Institut für Technische Chemie und Polymerchemie, Universität Karlsruhe, D-76128 Karlsruhe, Germany

Received 15 August 2007; received in revised form 21 November 2007; accepted 24 November 2007
Available online 14 January 2008

Abstract

This study addresses the catalytic reaction of NO_x and soot into N_2 and CO_2 under O_2-rich conditions. To elucidate the mechanism of the soot/NO_x/O_2 reaction and particularly the role of the catalyst α-Fe_2O_3 is used as model sample. Furthermore, a series of examinations is also made with pure soot for reference purposes. Temperature programmed oxidation and transient experiments in which the soot/O_2 and soot/NO reaction are temporally separated show that the NO reduction occurs on the soot surface without direct participation of the Fe_2O_3 catalyst. The first reaction step is the formation of CC(O) groups that is mainly associated with the attack of oxygen on the soot surface. The decomposition of these complexes leads to active carbon sites on which NO is adsorbed. Furthermore, the oxidation of soot by oxygen provides a specific configuration of active carbon sites with suitable atomic orbital orientation that enables the chemisorption and dissociation of NO as well as the recombination of two adjacent N atoms to evolve N_2. Moreover, carbothermal reaction, high resolution transmission electron microscopy and isotopic studies result in a mechanistic model that describes the role of the Fe_2O_3 catalyst. This model includes the dissociative adsorption of O_2 on the iron oxide, surface migration of the oxygen to the contact points of soot and catalyst and then final transfer of O to the soot. Moreover, our experimental data suggest that the contact between both solids is maintained up to high conversion levels thus resulting in continuous oxygen transfer from catalyst to soot. As no coordinative interaction of soot and Fe_2O_3 catalyst is evidenced by diffuse reflectance infrared Fourier transform spectroscopy a van der Waals type interaction is supposed.

Keywords: Simultaneous catalytic conversion; NO_x reduction; Soot oxidation; Mechanism; Fe_2O_3 catalyst; Oxygen transfer; Isotope labelling; DRIFTS; HRTEM

1. Introduction

Nitrogen oxides (NO_x) and soot particles produced by diesel engines can cause environmental and health problems. Hence, several techniques of exhaust after treatment have been developed in the past to minimize these emissions. For the removal of nitrogen oxides the selective catalytic reduction by NH_3 (SCR) and NO_x storage reduction catalysts (NSR) are currently the most favoured procedures, while for the elimination of soot so-called diesel particulate filters (DPFs) are taken into consideration. These technologies are described in detail in a recent review from Twigg [1] and are also summarised in a paper that we have published lately [2]. However, it should be noted that the procedures developed so far include either the removal of NO_x or soot. In contrast to that, relatively small attention has been given to the direct catalytic conversion of both pollutants into N_2 and CO_2. In this proposed technique, the trapped soot reacts with NO_x on a catalyst that is coated on the DPF system. In fact, basic examinations mainly performed with catalyst/soot powder mixtures have proven that this conversion exists even under oxidising conditions as present in diesel exhaust [2–16]. Moreover, these studies have shown that especially iron containing oxides are effective catalysts for the direct NO_x/soot conversion, e.g. "$Cu_{0.9}K_{0.1}Fe_2O_4$" [8], Fe_2O_3 [6,13], "$Fe_{1.9}K_{0.1}O_3$" [13] and Fe_2O_3/β-zeolite [2].

The mechanism of the catalytic NO_x/soot reaction in excess of oxygen has been addressed by the groups of Tomita and Teraoka. The latter group postulates a route, in which C(O) intermediates, that are originated from soot oxidation by NO_2 or O_2, react with adsorbed NO to form N_2 and CO_2 [17,18]. However, this mechanistic proposal is rather speculative as it is only based on global kinetic data and does not describe the role of the employed $CuFe_2O_4$ catalyst. In contrast to that, Tomita and co-workers [19] suppose activated carbon sites to be crucial for the reduction of NO. These sites are formed by the thermal desorption of reactive C(O) intermediates that, however, can partially be transformed into stable C(O) species leading to a

* Corresponding author. Tel.: +49 721 608 8090; fax: +49 721 608 2816.
E-mail address: kureti@ict.uni-karlsruhe.de (S. Kureti).

0926-3373/$ – see front matter © 2007 Elsevier B.V. All rights reserved.
doi:10.1016/j.apcatb.2007.11.024

decrease of soot reactivity. Following Tomita, the used Cu catalyst supports the soot oxidation and thus the production of the active carbon atoms.

Furthermore, a large number of papers has been published on the non-catalytic conversion of nitric oxide and carbon black, mainly in the field of coal chemistry. However, the majority of these studies has been carried out in the absence of oxygen [20,21], whereas the most detailed mechanism has been suggested by Teng et al. [22]. These authors suppose that NO is dissociatively adsorbed on two adjacent sites representing two carbon sites, a carbon site and a C(O) species, a very active carbon site and a C(O) species or two very active carbon sites. The NO adsorption leads to the formation of C(N) compounds that are subsequently converted into N_2 and two very active carbon sites. Furthermore, Yang et al. [23] and Suzuki et al. [24] have shown that C(N) surface complexes are also crucial for the evolution of N_2 when O_2 is present in the reaction of carbon black with NO. Additionally, both groups have observed an enhancement of the NO reduction by O_2 that is referred to the increased number of C(O) groups that decompose to form active carbon sites. Yang et al. have postulated that these carbon sites are activated by thermally stable C(O) complexes that are in close proximity [23]. Moreover, formation of more stable N species has also been reported for the NO_x/O_2/soot reaction, i.e. pyrrolic, pyridinic as well as NO and NO_2 containing fragments [25]. Additionally, the chemisorption of NO as well as N_2 formation on soot surface has been analyzed by Kyotani and Tomita using ab initio molecular orbital calculations [26].

The role of metal oxide catalysts in the soot/O_2 reaction has been investigated by the group of Moulijn [27,28] differentiating three types of mechanisms for the transfer of oxygen from catalyst to soot surface: (i) a redox mechanism in which only surface oxygen of the catalyst is transferred (Co_3O_4, Fe_2O_3), (ii) a redox mechanism combined with a spillover of oxygen (Cr_2O_3) and (iii) a ''classical'' redox mechanism in which lattice oxygen from the bulk of the catalyst is active (MoO_3, V_2O_5, K_2MoO_4).

The aim of the present study is (a) to advance the mechanism of the catalytic reaction of NO_x and soot into N_2 and CO_2 on Fe_2O_3 under oxygen rich conditions and (b) to elucidate the role of the catalyst in the activation of the soot. To achieve these objectives temperature programmed techniques, transient experiments, isotope labelling and surface analyses, i.e. high resolution transmission electron microscopy (HRTEM) and diffuse reflectance infrared Fourier transform spectroscopy (DRIFTS), are performed. The studies are carried out by using both pure soot and Fe_2O_3/soot mixtures.

2. Experimental

2.1. Preparation and characterisation of Fe_2O_3 catalyst and soot

The α-Fe_2O_3 catalyst used in this study is synthesized by polyvinyl alcohol technique as described previously [13]; the final calcination is carried out at 600 °C in air for 5 h. The crystalline structure is confirmed by powder X-ray diffraction that is performed at room temperature on a Siemens D 501 employing Ni filtered Cu Kα radiation. The BET surface area measured by multi-point Sorptomatic 1990 (Porotec) with N_2 as adsorbate is found to be 15 m^2/g. Moreover, for the HRTEM and some DRIFTS studies a nano-sized α-Fe_2O_3 sample is used that is prepared by dosing $Fe(CO_5)$ to a premixed lean H_2/O_2 flame [29]; the size of the primary particles ranges from 1 to 10 nm, while the BET surface area amounts to 130 m^2/g.

Table 1
Physical–chemical properties of the used C_3H_6 soot

BET surface area	91 m^2/g
Amount of adsorbed species	2.6 wt.%
Chemical composition[a,b]	98.8 wt.% C, 0.7 wt.% O, 0.5 wt.% H
Diameter of primary particles	20,. . .,100 nm

[a] The amount of adsorbed species is neglected.
[b] The soot is ashless.

The diesel model soot is prepared by burning a lean C_3H_6/O_2 mixture in a diffusion flame and is subsequently collected with a sinter metal filter. Detailed data about preparation have been reported recently [2], while the most important physical–chemical properties of the soot are summarised in Table 1.

2.2. Catalytic studies

For the catalytic examinations the iron oxide is blended with soot in the weight ratio of 27. The blending procedure is accurately performed by grinding the solids in a mortar that results in tight contact. To avoid discharge in the measurements the mixture is pressed to pellet with 40 MPa, granulated and sieved to a mesh size of 125–250 μm. Preliminary investigations demonstrate that pressing and granulating does not affect the activity of the mixture, whereas the initial grinding procedure is found to be the crucial step in the preparation. The tight contact mode is generally considered to be less representative for soot deposited in DPF systems [30], but in our opinion it is suitable for the intended basic examinations as reproducible conditions are simply provided. In each study a granulated mixture of 3.31 g is used that corresponds to 3.19 g Fe_2O_3 (20 mmol) and 0.12 g soot (10 mmol C). For reference purposes pure soot as well as pure Fe_2O_3 granules are also prepared, while the soot sample is diluted with 500 mg crushed quartz wool to avoid hot spots during oxidation.

The investigations are carried out by using temperature programmed oxidation (TPO) and transient experiments. In all these examinations the same laboratory bench is used that includes a quartz glass tube (i.d. 8 mm), in which the sample is fixed with quartz wool. The pipes of the bench are made of stainless steel and are heated to 150 °C. The inlet and outlet temperature of the feed is monitored by a K type thermocouple fitted directly in front of and behind the sample. For simplicity, the inlet temperature is exclusively noted throughout the paper as in all measurements a small difference of inlet and outlet temperature (<10 K) is observed only, even at maximum soot oxidation rates. In the examinations the total gas flow is kept at 500 cm^3/min (STP), while the feed is a blend of the pure components (Air Liquide) dosed from independent flow

controllers (MKS Instruments). A gas mixture that consists of 500 ppm NO, 6 vol.% O_2 and Ar as balance is used as standard feed. The gas analyses are performed by the following techniques: chemiluminescence for NO_x (CLD EL-ht, Eco Physics), gas chromatography coupled with thermal conductivity detection for N_2 (GC/TCD, RGC 202 with packed columns Haye Sep Q 60 and mol sieve 5 Å, Siemens), non-dispersive infrared spectroscopy for N_2O, CO and CO_2 (NDIR, Uras 10 E, Hartmann & Braun) and magnetomechanics for O_2 (Magnos 6 G, Hartmann & Braun). In transient and isotopic study, NO_x, N_2, N_2O, O_2 and H_2O are monitored by chemical ionisation mass spectrometry (CIMS, Airsense 500, V&F). Moreover, in the transient investigations N_2 is detected by passing a part of the reactor effluent on a Pt oxidation catalyst that is heated at 400 °C and that is additionally fed with O_2 such that the potentially present CO is completely converted resulting in an unequivocal assignment of $m/z = 28$. Here, CO is monitored by analysing another part of the effluent using NDIR.

2.2.1. TPO and carbothermal studies

TPO studies are performed with pure soot as well as the Fe_2O_3/soot mixture. The sample is heated to 150 °C in Ar flow; then, the feed is added and the temperature is linearly increased to 650 °C at the rate of 1.5 K/min. In order to investigate the effect of NO and NO_2 on the catalytic soot/NO_x/O_2 reaction several gas mixtures (GM) are used in addition to the standard feed. These mixtures are listed in Table 2. A temperature programmed reaction of the Fe_2O_3/soot mixture is also carried out without NO_x and O_2 at a rate of 10 K/min up to a final temperature of 1000 °C (carbothermal study); for comparison a corresponding measurement is also conducted with the pure catalyst.

Furthermore, some TPO blank experiments are performed in the absence of soot to study the activity of the Fe_2O_3 catalyst in NO oxidation, CO oxidation and NO/CO reaction. The former conversion is performed with the standard feed, while for the latter ones the gas mixture consists of 0 or 500 ppm NO, 0 or 7000 ppm CO, 6 vol.% O_2 and Ar as balance.

2.2.2. Transient studies

To study the direct reaction of NO with soot the soot/NO_x/O_2 conversion is temporally separated into the soot/O_2 and soot/NO reaction. This separation is achieved by stringing together different transient reaction steps. The examinations are carried out in the absence as well as in the presence of the Fe_2O_3 catalyst and are done under isothermal conditions, i.e. at 400 °C with catalyst and at 560 °C without catalyst. In the 1st phase the soot is oxidised by O_2 (5.0 vol.% O_2, 95 vol.% Ar) up to a defined conversion level, while in the 2nd stage the dosage of O_2 is stopped and the sample is flushed with Ar. After complete desorption of CO_x, the 3rd regime is started by switching to a gas mixture of 500 ppm NO in Ar. In the final period the remaining soot is completely oxidised by a TPO performed with 5.0 vol.% O_2 in Ar up to 650 and 715 °C, respectively, at a rate of 10 K/min.

Table 2
Gas mixtures (GM) used in the TPO experiments[a,b]

GM 1[c]	500 ppm NO, 6.0 vol.% O_2
GM 2	250 ppm NO, 250 ppm NO_2, 6.0 vol.% O_2
GM 3	2500 ppm NO, 6.0 vol.% O_2
GM 4	6000 ppm NO, 6.0 vol.% O_2
GM 5	6.0 vol.% O_2

[a] Ar is used as balance.
[b] The NO and NO_2 concentrations refer to the bypass heated at 150 °C.
[c] GM 1 represents the standard gas mixture.

2.2.3. Isotopic study

A TPO examination of the catalyst/soot blend is performed with $^{18}O_2$ labelled oxygen (Linde) to investigate the oxygen transfer from the catalyst to soot. To reduce the amount of $^{18}O_2$ the reaction conditions are modified as compared to the standard TPO experiment (Section 2.2.1), i.e. a mixture of 58 mg Fe_2O_3 (0.36 mmol) and 2.2 mg soot (0.18 mmol C) is used, while the $^{18}O_2$ concentration is 0.19 vol.% and Ar is taken as balance. The measurement is conducted in the range from 200 to 875 °C at a heating rate of 20 K/min; the total flow is 500 cm^3/min (STP). Furthermore, a HTPR study (temperature programmed reduction by H_2) is subsequently performed to balance the mass of oxygen. After the TPO, the catalyst is cooled to 200 °C in Ar and is exposed to a mixture of 10 vol.% H_2 and 90 vol.% Ar. The temperature is then increased with a rate of 20 K/min to the final temperature of 975 °C which is held for 5 min.

2.3. HRTEM studies

HRTEM investigations are performed to follow the contact between the catalyst and soot with proceeding conversion. For the accurate discrimination of both solids the nano-sized Fe_2O_3 catalyst is used. Its mixture with soot is prepared as described in Section 2.2 and the fresh samples are then exposed to a TPO using gas mixture 5. After reaching a soot conversion of 40, 70, 90 and 97%, respectively, the reaction is quenched by stopping the dosage of O_2 and rapidly cooling to room temperature. The HRTEM pictures are taken with a Philips CM200 FEG.

2.4. DRIFTS studies

DRIFTS studies are made to investigate the interaction between the catalyst and soot surface. The investigations are performed by using soot and other model soot samples with prominent reflectance (phthalic acid, 9-phenyl-2,3,7-trihydroxy-6-fluorone, anthracene, chinone and 9(10H)-anthracenone) and are conducted in the absence as well as in the presence of the catalyst. The catalytic mixtures are prepared as mentioned above, i.e. the molar ratio of catalyst/soot is 2. The spectra are recorded on a Nicolet 5020 FTIR spectrometer (Thermo Electron) that is equipped with a MCT detector and DRIFTS optics (Thermo Mattson). The IR cell made of stainless steel contains a KBr window and is connected to a gas-handling system. The spectra are recorded at 50 °C in a N_2 flow of 500 cm^3/min (STP) without special pre-treatment of the

sample. The data are collected in the range from 650 to 4000 cm^{-1} with an instrument resolution of 4 cm^{-1}, while 1500 scans are accumulated to a spectrum. A mirror fitted on the sample cup is used as reference. During the measurements the spectrometer as well as the DRIFTS optics are purged with nitrogen to avoid diffusion of air into the system.

3. Results and discussion

3.1. Mechanism of the catalytic reaction of NO_x and soot on Fe_2O_3 in presence of O_2

The TPO data of the soot as well as the Fe_2O_3/soot mixture that are obtained with different gas compositions are summarised in Table 3. Additionally, the respective traces recorded in the standard feed (GM 1) are depicted in Figs. 1 and 2. The results evidence the simultaneous production of CO, CO_2, N_2 and N_2O, whereas in presence of the catalyst a CO peak is also observed at relatively low temperature (ca. 280 °C). Furthermore, the TPO profiles of the catalytic conversion are significantly shifted to lower temperatures, e.g. the temperature at maximum CO_2 concentration (T_m) is decreased from 580 to 420 °C. Additionally, the catalyst markedly enhances the conversion of NO_x as well as the selectivity of N_2. By the use of pure soot a total amount of 28 μmol N_2 is formed (overall N_2 selectivity: 55%), while in presence of the catalyst it is 83 μmol (overall N_2 selectivity: 86%). The inset of Figs. 1 and 2 shows that the reduction of NO_x fairly corresponds to the formation of N_2 and N_2O, i.e. the mass of nitrogen is balanced. However, even in presence of the catalyst the NO_x reduction has to be considered as a side reaction of the soot/O_2 conversion as indicated by the total amounts evolved in TPO ($(n(CO) + n(CO_2))/(n(N_2) + n(N_2O)) = 100$).

Moreover, it is obvious that CO is only formed in trace amounts when Fe_2O_3 is present, whereas high concentrations up to 0.43 vol.% are found without catalyst. The overall molar ratio of CO_2:CO is 0.85 in absence, but 250 in presence of the catalyst. The TPO data of the catalytic CO/O_2 reaction indicate

Table 3
Total molar amounts of CO, CO_2, N_2 and N_2O formed in TPO as well as corresponding temperature at peak CO_2 concentration (T_m): TPO experiments are performed with and without Fe_2O_3 catalyst using different gas mixtures[a,b]

	$n(N_2)$ (μmol)	$n(N_2O)$ (μmol)	$n(CO)$ (mmol)	$n(CO_2)$ (mmol)	T_m (°C)
Fe_2O_3/soot					
GM 1	83	14	0.04	9.96	420
GM 2	83	14	0.04	9.96	420
GM 3	103	29	0.05	9.95	383
GM 4	160	58	0.05	9.95	370
GM 5	–	–	0.05	9.95	420
Pure soot					
GM 1	28	23	5.4	4.6	580
GM 2	28	23	5.4	4.6	580
GM 5	–	–	5.0	5.0	580

[a] Conditions: m(soot) = 0.12 g (10 mmol C), $m(Fe_2O_3)$ = 3.19 g (20 mmol), F = 500 cm^3/min (STP), $\Delta T/\Delta t$ = 1.5 K/min.
[b] The composition of the gas mixtures is listed in Table 2.

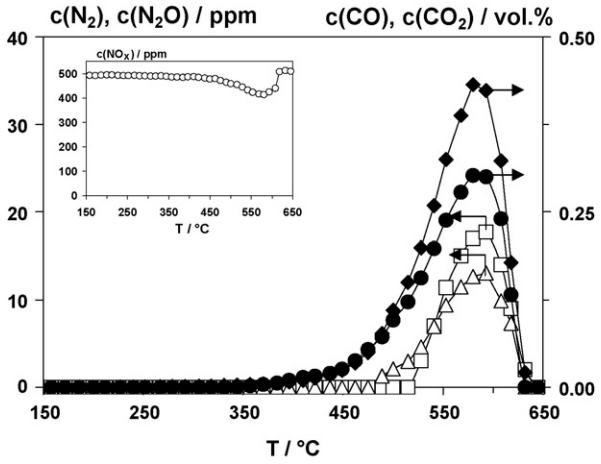

Fig. 1. Concentration of N_2 (□), N_2O (△), CO (◆) and CO_2 (●) in the non-catalytic soot/NO_x/O_2 reaction using the standard feed. The inset shows the corresponding concentration of NO_x. Conditions: m(soot) = 0.12 g (10 mmol C), c(NO) = 500 ppm, $c(O_2)$ = 6.0 vol.%, Ar balance, F = 500 cm^3/min (STP), $\Delta T/\Delta t$ = 1.5 K/min.

a pronounced activity of the Fe_2O_3, i.e. complete conversion of CO is obtained already at 250 °C. From this result we conclude that CO formed in catalytic soot/NO_x/O_2 reaction is subsequently oxidised on Fe_2O_3 and therefore only a very small concentration of CO is observed. It may be speculated that these trace amounts are associated with the soot oxidation occurring at the back part of the soot/Fe_2O_3 bed leading to reduced residence time and thus incomplete CO conversion. The TPO in which NO is additionally dosed to the CO/O_2/Ar feed proves that NO_x is not reduced by CO on the pure catalyst under O_2-rich conditions, i.e. neither N_2 nor N_2O are formed (Fig. 3). These reference data provide evidence that the NO_x reduction obtained in catalytic soot/NO_x/O_2 conversion is not associated with the reaction of NO_x and CO on the Fe_2O_3 catalyst. Hence, from these results we derive that even in the presence of the

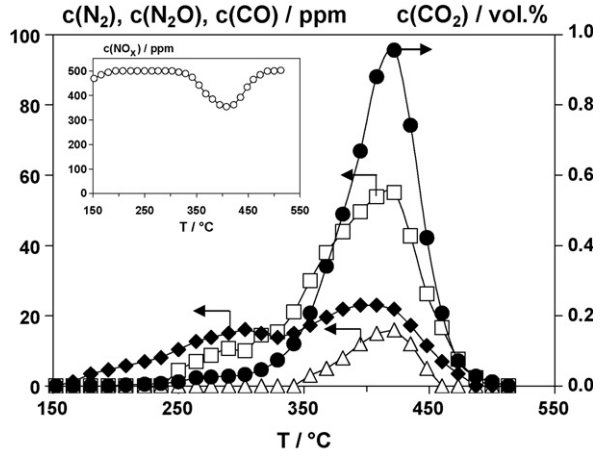

Fig. 2. Concentration of N_2 (□), N_2O (△), CO (◆) and CO_2 (●) in the catalytic soot/NO_x/O_2 reaction on Fe_2O_3 using the standard feed. The inset shows the corresponding concentration of NO_x. Conditions: $m(Fe_2O_3)$ = 3.19 g (20 mmol), m(soot) = 0.12 g (10 mmol C), c(NO) = 500 ppm, $c(O_2)$ = 6.0 vol.%, Ar balance, F = 500 cm^3/min (STP), $\Delta T/\Delta t$ = 1.5 K/min.

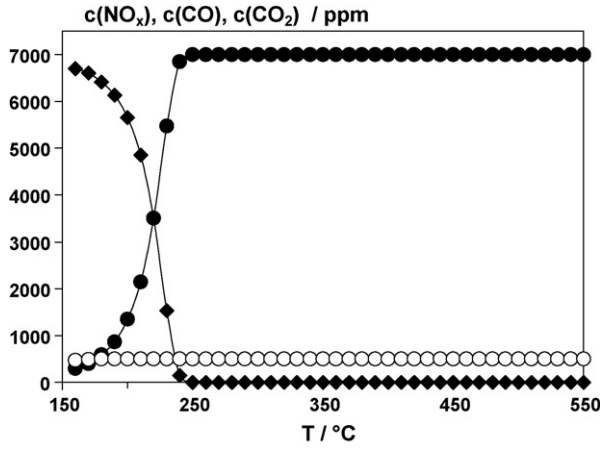

Fig. 3. Concentration of NO_x (○), CO (◆) and CO_2 (●) in the catalytic CO/NO_x/O_2 reaction on pure Fe_2O_3. Conditions: $m(Fe_2O_3)$ = 3.19 g (20 mmol), c(CO) = 7000 ppm, c(NO) = 500 ppm, $c(O_2)$ = 6.0 vol.%, Ar balance, F = 500 cm^3/min (STP), $\Delta T/\Delta t$ = 1.5 K/min.

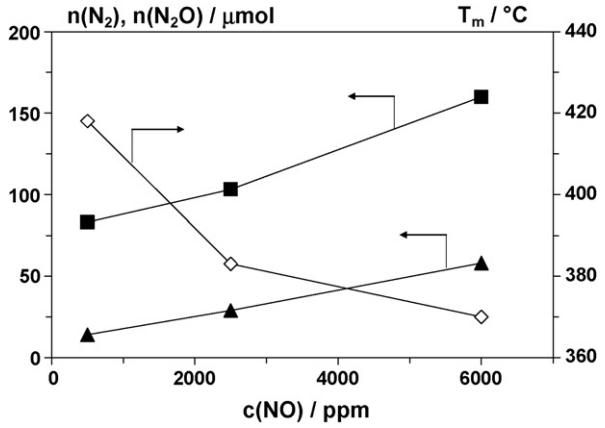

Fig. 4. Catalytic soot/NO_x/O_2 reaction on Fe_2O_3: effect of the inlet concentration of NO on the temperature at peak CO_2 concentration (T_m, ◇) as well as on the total molar amount of N_2 (■) and N_2O (▲). Conditions: $m(Fe_2O_3)$ = 3.19 g (20 mmol), m(soot) = 0.12 g (10 mmol C), c(NO) = 500, 2500 or 6000 ppm, $c(O_2)$ = 6.0 vol.%, Ar balance, F = 500 cm^3/min (STP), $\Delta T/\Delta t$ = 1.5 K/min.

catalyst NO_x is exclusively reduced on the soot surface as observed in the non-catalytic conversion (Fig. 1).

When gas composition 2 (each 250 ppm NO and NO_2) and 5 (6 vol.% O_2) are employed in catalytic and non-catalytic reaction the same values of T_m are obtained as for the standard feed (GM 1). We therefore draw the conclusion that NO_2 does not contribute substantially to the soot oxidation under the reaction conditions established here. This seems to disagree with the literature [31], but is obviously referred to the relatively high W_{soot}/F_{NO_x} ratio that amounts to 29 gs/cm^3 in the beginning of the reaction. It should be noted that in the NO oxidation on the Fe_2O_3 catalyst thermodynamic NO_2 concentrations are achieved at 350 °C regardless of gas mixture 1 and 2.

Moreover, in the catalytic soot/NO_x/O_2 reaction the same formation of NO_2 is observed with GM 1 and 2 above 275 °C, whereas it is significantly below the thermodynamic limit. This result indicates an appreciable conversion of NO_2 and soot into NO and CO_x as reported in the literature [31]. For example, at 300 °C where no reduction of NO_x in N_2 is observed the amount of NO_2 is 45 ppm, while without soot it is 305 ppm. Nevertheless, the observed NO_2/soot reaction does not result in a significant shift of T_m as discussed above. Furthermore, the same traces of N_2 and N_2O are obtained when GM 1 and 2 are used in catalytic and non-catalytic soot/NO_x/O_2 reaction showing that NO_x reduction is also not affected by the amount of NO_2 initially present.

Contrary, Fig. 4 shows that the increase of the inlet concentration of NO in the gas phase (GM 3 and 4) results in the enhancement of the catalytic soot/NO_x/O_2 reaction, i.e. the production of N_2 and N_2O grows and T_m shifts towards lower temperatures. Since it is well-known that NO_x [21,32] as well as O_2 [33] chemisorb on the soot surface, the mounted conversion of NO_x is very likely associated with the competitive adsorption of O_2 and NO on the soot surface. The uptake of NO seems to be favoured with increasing ratio of NO/O_2 thus resulting in a higher NO reduction rate. However, the growing NO:O_2 ratio also leads to a clear decrease in the molar proportion of N_2/N_2O (5.9 for GM 1, 3.6 for GM 3 and 2.8 for GM 4). Furthermore, it is evident that the shift of T_m refers to both the decrease of W_{soot}/F_{NO_x} (initially: 29, 5.8 and 2.4 gs/cm^3) and the increased fraction of NO_2 formed on the catalyst. The amounts of NO_2 produced in catalytic soot/NO_x/O_2 reaction are again compared at 300 °C where NO_x is not yet reduced to N_2, i.e. 45 ppm NO_2 for GM 1, 480 ppm for GM 3 and more than 750 ppm for GM 4. For the latter feed more detailed data are not available as higher concentrations of NO_2 cannot be measured reliably with the CLD employed. However, these results clearly indicate that the growing inlet concentration of NO leads to an outstanding increase in the NO_2 fraction that is considered to be crucial for the acceleration of the soot oxidation in gas mixtures 3 and 4. Furthermore, it should be taken into account that the increased proportion of NO_2 enhances the formation of CC(O) groups on the soot surface [31], whereas such groups are also produced in the reaction of soot with O_2. In accordance with the literature [22–24] the decomposition of these surface complexes leads to the formation of coordinatively unsaturated carbon atoms (C*, Eq. (1)) that are considered to be the active sites for the chemisorption of NO.

$$CC(O) \rightarrow C^* + CO(g) \quad (1)$$

It is generally accepted that the evolution of N_2 is assigned to the dissociation of adsorbed NO that takes place on two adjacent C* sites producing C(N) and C(O) species. Finally, the combination of two neighbouring C(N) groups leads to N_2 and regeneration of the C* sites [20–22]. This is in accordance with the above stated result that the increased NO reduction presented in Fig. 4 is also referred to the mounted production of NO_2 on the Fe_2O_3 catalyst that enhances the number of CC(O) complexes and C* sites, respectively. On the other hand we rule out that NO_2 is directly involved in the formation of N_2 [23]. As discussed above, NO_2 is much more reactive towards soot oxidation than NO. In this conversion NO_2 rapidly transfers one of its oxygen atoms to the soot surface that leads to the production of NO and CC(O) species. This fast abstraction of oxygen is assigned to the relatively low bonding dissociation

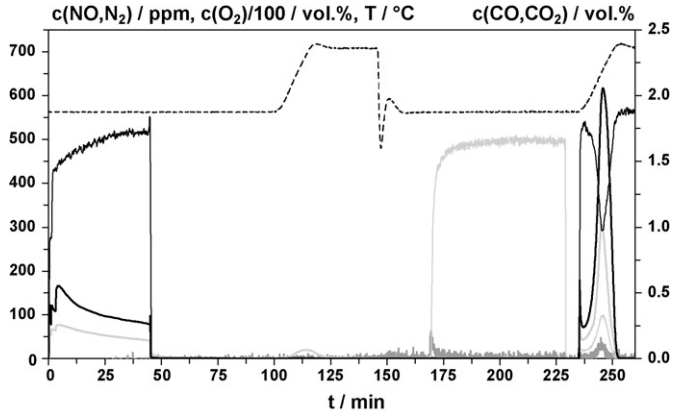

Fig. 5. Concentration of O_2 (–), CO (—), CO_2 (▬), NO (—) and N_2 (▬) as well as temperature (- - -) in the transient study of pure soot. Conditions: m(soot) = 0.12 g (10 mmol C), F = 500 cm^3/min; 1st regime: $c(O_2)$ = 5.0 vol.%, c(Ar) = 95 vol.%; 2nd: c(Ar) = 100 vol.%; 3rd: c(Ar) = 100 vol.%, $\Delta T/\Delta t$ = 10 K/min; 4th: c(NO) = 500 ppm, Ar balance; 5th: $c(O_2)$ = 5.0 vol.%, c(Ar) = 95 vol.%, $\Delta T/\Delta t$ = 10 K/min.

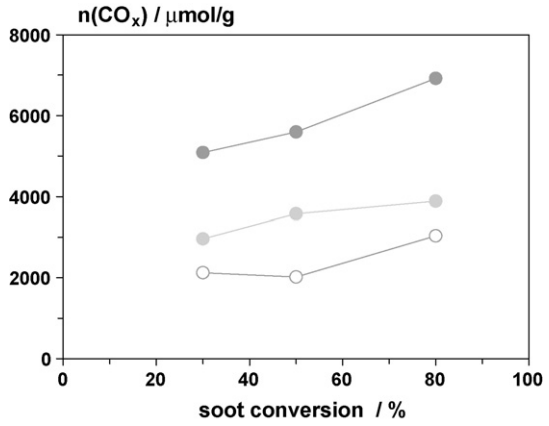

Fig. 6. Transient study of pure soot: effect of the conversion of soot in the 1st phase on the number of CO_x directly desorbed after oxidation (○) and released by TPD (●); the darkly grey circles (●) represent the sum of both species. The amounts of CO_x refer to the mass of soot that remains after 1st phase of the experiment; conditions are described in Fig. 5 and Section 2.2.2.

enthalpy that amounts to 306 kJ/mol for gaseous NO_2 [34]. Moreover, it is obvious that the oxygen transfer from NO to soot results in the formation of nitrogen and takes place at elevated temperatures due to the higher dissociation enthalpy that is 634 kJ/mol for gaseous NO [34].

To obtain deeper insight into the reaction of NO and soot transient studies are conducted. They are firstly performed without catalyst and the soot is oxidised in the initial stage to a conversion level of 75%. However, after complete CO_x desorption (2nd stage) the exposure to NO only leads to a very little N_2 formation (max. 25 ppm) that is found to be within the analytical limits. Hence, for the detailed examination of the effect of decomposing CC(O) species on NO reduction a TPD in Ar flow is performed up to 715 °C subsequent to the 2nd phase and hereafter the sample is cooled to the initial temperature. This additional step is employed in the following experiments in which the conversion of soot (1st stage) is varied to 30, 50 and 80%. In order to clarify the experimental approach a full transient experiment is exemplarily illustrated for the soot that is converted to 50% (Fig. 5); a very typical feature is the pronounced N_2 peak always observed at the beginning of the NO exposure.

The results of the transient experiments without catalyst show that the amount of CO_x desorbing in the 2nd and subsequent TPD phase increases with the conversion of soot, whereas the abundance of CO released by TPD is always higher than that desorbed in the isothermal stage (Fig. 6); note that throughout the paper the given molar amounts are related to the mass of soot that remains after the initial O_2 treatment. Furthermore, Fig. 7 indicates a linear relation between the amount of NO reacted in the 4th stage and the number of CO_x totally released before. Additionally, the more CO_x desorbs the more NO directly converts into N_2. This substantiates the formation of active carbon sites by decomposition of oxygen containing surface species as presented in Eq. (1). Moreover, the results of our transient studies clearly show that N_2 is rapidly evolved in the NO exposure, but after reaching a maximum it goes down to zero. This inhibition is not related to the blocking of active sites by oxygen originated from NO dissociation as the transient experiments indicate quantitative release of the oxygen in the form of CO and CO_2. Additionally, our data provide evidence that the consumed NO is not completely converted into N_2. A significant proportion of nitrogen remains on the soot surface that ranges from 40 to 63% of the reacted NO and the amount declines with increasing abundance of CO_x desorbed before. The accumulation is substantiated by final TPO in which the soot is totally oxidised, whereby the N containing species are quantitatively released forming N_2 and NO (Figs. 5 and 7). It should be mentioned that the remaining nitrogen is not removed by a TPD performed up to 715 °C. We therefore assume that these nitrogen species are attributable to relatively stable components, such as pyrrolic, pyridinic and pyridonic fragments [25,35]. This accumulation of nitrogen obviously reduces the number of active carbon sites,

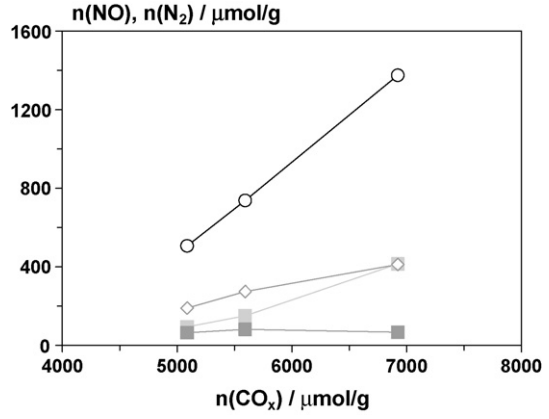

Fig. 7. Transient study of pure soot: effect of the number of CO_x totally desorbed in isothermal and TPD phase on the consumption of NO (○), on the formation of N_2 in NO exposure (■) and TPO (■) and on the release of NO in TPO (◇). The given amounts refer to the mass of soot that remains after 1st phase of the experiment; conditions are described in Fig. 5 and Section 2.2.2.

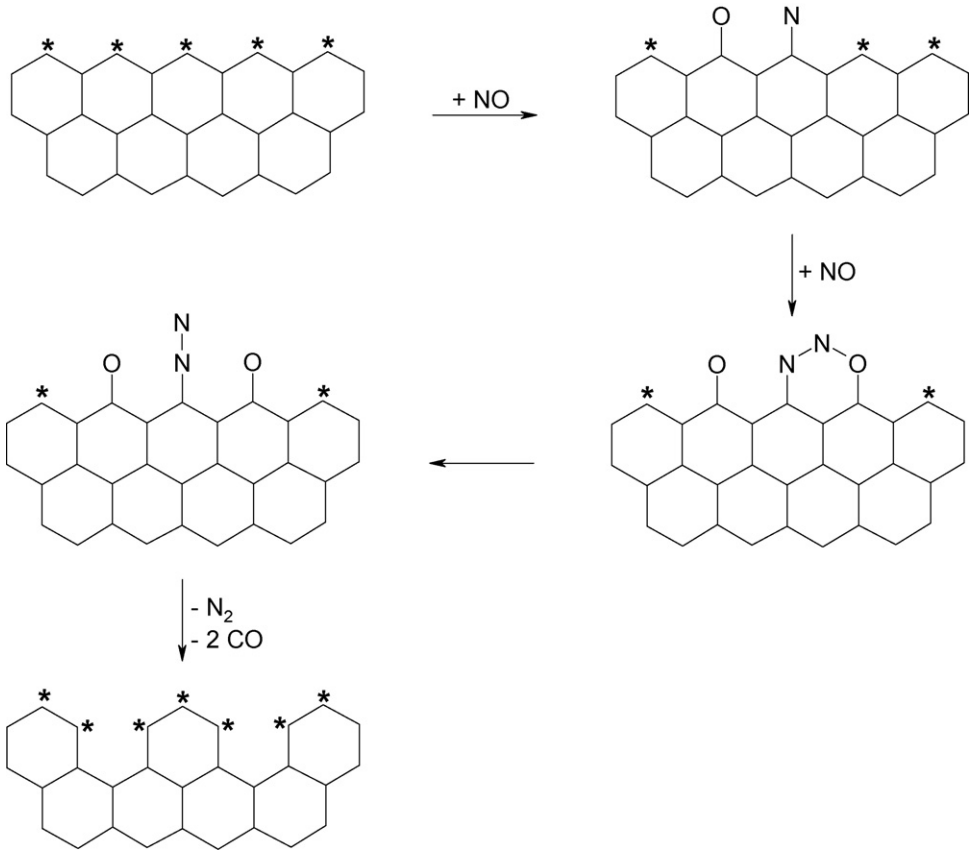

Fig. 8. Model for the N_2 formation in NO/soot reaction [26] and for the inhibition of the N_2 production observed in the transient studies. The edge C atoms on the upper side are unsaturated that is indicated by the asterisk, while the other C atoms are terminated with H atoms; the C body is polyaromatic.

but it does not entirely explain the inhibition observed in NO exposure. Quantum-mechanical calculations from Kyotani and Tomita [26] show that in NO/soot reaction three neighbouring active C* sites located at the edge of the carbon network are preferably involved in the evolution of N_2 (Fig. 8). The chemisorption of a first NO molecule leads to formation of C(O) and C(N) groups, while the attack of a second NO results in a six-membered ring including a C(NNO) sequence. After breakage of the (N–O) and (C–N) bonds N_2 forms. Advancing this reasonable mechanistic model, the following desorption of the C(O) groups, as observed in our transient examinations, should lead to new active carbon sites (Fig. 8). However, the resulting configuration does not show three neighbouring C* sites that reveal appropriate atom orbital orientation as in the starting molecule. Thus, the pre-condition for the formation of N_2 is no more satisfied. The importance of suitable geometry of the participating carbon orbitals is evident and is also reported for the soot/O_2 reaction [36]. Hence, we draw the conclusion that the lack of suitable spatial arrangement of active carbon sites is the main reason for the inhibition obtained in NO exposure. Nevertheless, we do not exclude adsorption or even dissociation of NO on the formed carbon sites as well as rearrangement processes of the soot surface.

In contrast to pure soot the transient examinations of the Fe_2O_3/soot mixture are not performed with the intermediate TPD. Preliminary studies have shown that carbothermal reaction takes place in the TPD stage that leads to consumption of the active carbon sites thus completely suppressing the NO/soot reaction. In the 1st phase soot conversions of 34, 48 and 65% are adjusted; the experiment with 34% soot conversion is exemplarily presented in Fig. 9. From these traces it is obvious that in NO exposure a similar N_2 profile is observed as without catalyst, i.e. a rapid N_2 formation followed by inhibition of the soot/NO reaction. The relationship between the amount of CO_x

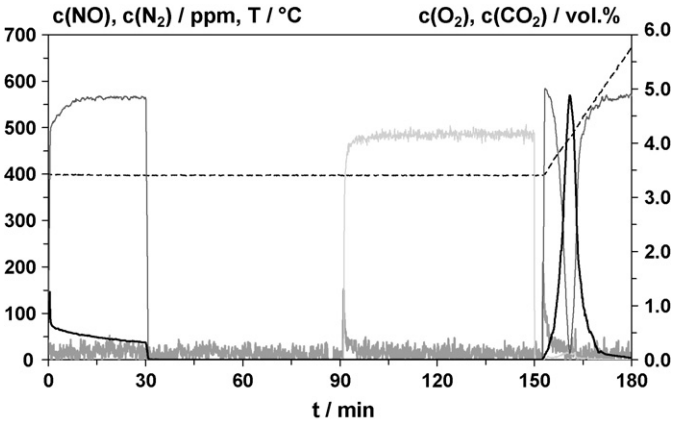

Fig. 9. Concentration of O_2 (–), CO_2 (▬), NO (▬) and N_2 (▬) as well as temperature (- - -) in the transient study of the Fe_2O_3/soot mixture. Conditions: m(soot) = 0.12 g (10 mmol C), $m(Fe_2O_3)$ = 3.19 g (20 mmol), F = 500 cm^3/min; 1st regime: $c(O_2)$ = 5.0 vol.%, c(Ar) = 95 vol.%; 2nd: c(Ar) = 100 vol.%; 3rd: c(NO) = 500 ppm, Ar balance; 4th: $c(O_2)$ = 5.0 vol.%, c(Ar) = 95 vol.%, $\Delta T/\Delta t$ = 10 K/min.

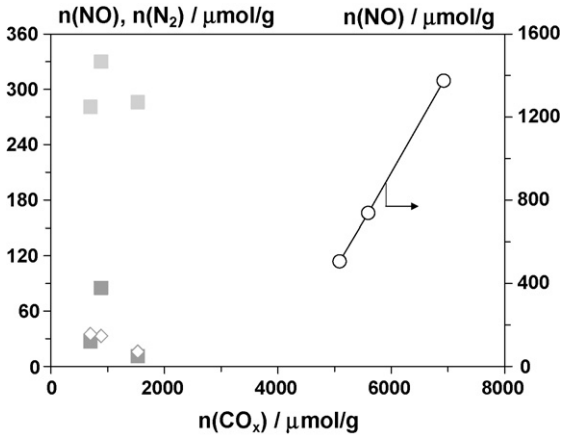

Fig. 10. Transient study of the Fe_2O_3/soot mixture: effect of the number of CO_x desorbed in isothermal phase on the formation of N_2 in NO exposure (■, no correction is made regarding reoxidation of Fe_2O_3) and TPO (■) and on the release of NO in TPO (◇). The given amounts refer to the mass of soot that remains after 1st phase of the experiment; conditions are described in Fig. 9 and Section 2.2.2. For comparison the dependence of consumption of NO from CO_x desorbed from pure soot (○) is also shown; these data are taken from Fig. 7.

desorbed and NO subsequently converted (400 °C) is shown in Fig. 10 indicating much lower CO_x release than in the studies conducted without catalyst (560 °C); the difference of the NO conversion obtained in the catalytic experiments is in the range of the reproducibility. As a consequence, a smaller number of active carbon sites with appropriate orientation of the atomic orbitals form which leads to a limited NO conversion. Furthermore, in the 2nd phase, in which the catalyst/soot mixture is flushed, CO_2 is solely monitored, whereas for pure soot a molar CO_2/CO ratio of 7 is found in desorption at 400 °C. The missing carbon monoxide is referred to the reaction of the Fe_2O_3 catalyst with desorbing CO that leads to the evolution of CO_2 and partial reduction of the catalyst. This conversion is proven by a blank experiment in which the catalyst is exposed to 330 ppm CO in Ar at 400 °C resulting in complete CO oxidation. Moreover, after CO treatment and subsequent flushing the catalyst is reoxidised by 500 ppm NO in Ar to form selectively N_2. Hence, this reaction has to be accounted for the interpretation of the N_2 production occurring in NO exposure. Assuming the same CO_2/CO ratio as for pure soot we derive that between 50 and 80% of the N_2 evolved is associated with the reoxidation of the catalyst. Furthermore, as observed for the pure soot a significant amount of the NO reacted with the soot (40–90%) is accumulated (Fig. 10); NO is not adsorbed at 400 °C on the Fe_2O_3 catalyst as shown in a preliminary investigation.

Moreover, the remaining N species are removed from the soot by final TPO. However, in opposite to the pure soot, N_2 is rapidly formed in the beginning of the TPO step (Fig. 9), while the evolution of NO follows the CO_2 profile as observed for pure soot. This observation shows that in the transient catalytic study other N species are formed that immediately react with O_2 upon heating. It is evident that these species reveal neighbouring N atoms that, however, are not capable of forming N_2 at 400 °C. Furthermore, we have found that the accumulated nitrogen is not converted into N_2 when a TPD up to 650 °C or isothermal O_2 exposure (400 °C) are carried out instead of TPO. Nevertheless, in both treatments NO is released, whereas the most part of the N containing species remains on the soot, i.e. 79% after TPD and 64% after isothermal O_2. The observed evolution of NO be associated with the decomposition of NO containing surface complexes that are reported in the literature [25]; for instance, such species could involve NO that is linearly bound to an active carbon site or that bridges two carbon sites [26]. Moreover, the significant stability of the retaining N species towards thermal treatment and O_2 exposure (400 °C) is likely associated with a saturated carbon coordination sphere, i.e. no C* sites are present in proximity that might react with O_2 causing release of N_2 and/or NO. We suppose that these N containing species represent cyclic systems with neighbouring N atoms. An indication for this supposition might be provided by the MO calculations from Kyotani and Tomita [26]. They have reported pyridinic species on which NO is chemisorbed resulting in a five-membered (C–O–N–N–C) ring. This structure is shown to be drastically less favoured for the evolution of N_2 as compared to the six-membered compound discussed above (Fig. 8).

Furthermore, we interpret the inhibition of the NO/soot reaction on Fe_2O_3 in the same way as for the non-catalytic conversion, i.e. the consumption of the active carbon sites with appropriate spatial orientation of the atomic orbitals. However, in contrast to the transient investigations, the TPO studies performed with and without catalyst show continuous NO/soot reaction (Figs. 1 and 2) indicating that the soot/O_2 conversion is crucial for the NO reduction. Therefore, we conclude that in the presence of O_2 appropriate arrangements of reactive carbon sites are permanently produced avoiding the inhibition of the NO conversion; note that this activation of soot surface takes place in the initial stage of transient studies in which the soot is exposed to O_2. This interpretation is in line with a previous study in which we have shown suppression of catalytic NO reduction in the absence of O_2 [13]. However, we have also demonstrated in that paper that a high excess of oxygen is counterproductive for the soot/NO reaction as the soot/O_2 reaction is more enhanced then.

Furthermore, another significant difference between the TPO and transient studies is the suppression of N_2O production in the latter. In our opinion a plausible mechanism for the formation of nitrous oxide is the reaction of a C(N) species with adsorbed or gas-phase NO. However, the explanation for the absence of N_2O is difficult, whereas it may also be speculated that nitrous oxide is formed in trace amounts below the analytical limit. Finally, it should be noticed that ex as well as in situ DRIFTS analysis of the N containing surface groups formed in NO exposure did not provide clear absorption bands and hence these data are not useful for discussion. This failure is referred to the low reflectivity of soot and Fe_2O_3/soot mixture as well as to the low surface concentration of the formed nitrogen complexes.

3.2. Mechanism of the soot activation by the Fe_2O_3 catalyst

From the above stated discussion a tight relationship of soot/NO and soot/O_2 reaction becomes evident. However, the former

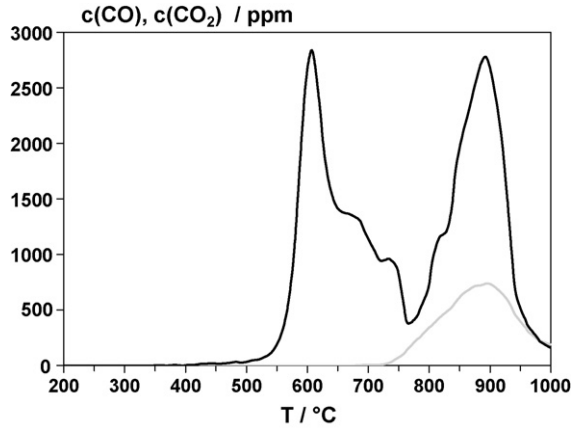

Fig. 11. Concentration of CO (═) and CO_2 (━) in the carbothermal reaction of the Fe_2O_3/soot mixture. Conditions: $m(Fe_2O_3)$ = 3.19 g (20 mmol), m(soot) = 0.12 g (10 mmol C), c(Ar) = 100 vol.%, F = 500 cm^3/min (STP), $\Delta T/\Delta t$ = 10 K/min.

is found to be a side reaction and is not directly affected by the catalyst. Therefore, the role of the catalyst is firstly examined without dosing NO. The contact between Fe_2O_3 and soot is investigated by carbothermal reaction. This conversion results in two CO_2 peaks located at 610 and 895 °C with an additional evolution of CO in the latter range (Fig. 11). As the stoichiometric ratio of Fe_2O_3/C is 2 and almost the total amount of soot is consumed, it is evident that the catalyst is reduced to FeO. In contrast to that, the PXRD pattern recorded hereafter exclusively indicates reflexes of Fe and Fe_3O_4. However, this result is in fair agreement with thermodynamics that show the disproportion of FeO below ca. 555 °C [37]. We assume that the first CO_2 feature is principally referred to the formation of Fe_3O_4 as reported for the reaction of Fe_2O_3 with H_2 [38] and CO [39]. Furthermore, since the pure catalyst starts releasing oxygen at 900 °C only the evolution of CO_x observed in carbothermal reaction is not related to the reaction of soot with gas-phase oxygen originated from the catalyst by desorption or decomposition, but with the diffusion of oxygen from the iron oxide to soot. Moreover, the thermal desorption of oxygen containing groups originally present on the soot surface is to be neglected (Table 1). Additionally, as the soot is almost completely converted we deduce a continuous oxygen transfer from the catalyst to the soot and thus maintenance of the contact between both solids. The latter conclusion is also supposed for the reaction in presence of gas-phase oxygen as shown by the HRTEM studies performed with the mixture of the nano-sized Fe_2O_3 and soot. The micrographs show that the contact of catalyst and soot is maintained at soot conversions of 40, 70 and even 90%. For demonstration Fig. 12 displays the HRTEM pictures of the fresh blend and the mixture with 90% conversion in TPO. Furthermore, it is discernible that the spherical shape as well as the mean diameter of the soot primary particles do not change in the oxidation and the particles only collapse if nearly total conversion is reached. At a conversion of 97% no more primary particles of soot or resulting fragments are observed in the micrograph. Moreover, in SEM studies performed with the bulk-Fe_2O_3/soot mixture a change in mean diameter of primary particle is not obtained as well. Thus, we deduce no different oxidation mechanism for the nano-sized and bulk-Fe_2O_3.

The DRIFT spectra of the pure soot and the fresh mixture of nano-sized Fe_2O_3 and soot are depicted in Fig. 13, whereas they do not show a significant difference. This observation is in line with results from Mul et al. [27]. Fig. 13 shows the spectra that are recorded with the nano-sized Fe_2O_3 as it provides well resolved bands. The DRIFTS features of the soot are referred to vibrations of typical functional groups and are assigned in Table 4 [31,40–42]. However, the bands of the soot are broad and therefore a partial shift by interaction with the catalyst cannot be excluded. In contrast to that, well resolved features are obtained with model soot samples, whereas for 9(10H)-anthracenone, anthracene, chinone and 9-phenyl-2,3,7-trihydroxy-6-fluorone no change in the spectrum is observed in presence of the catalyst; only for phthalic acid a slight shift of the carboxyl bands towards lower wavenumbers (ca. 30 cm^{-1})

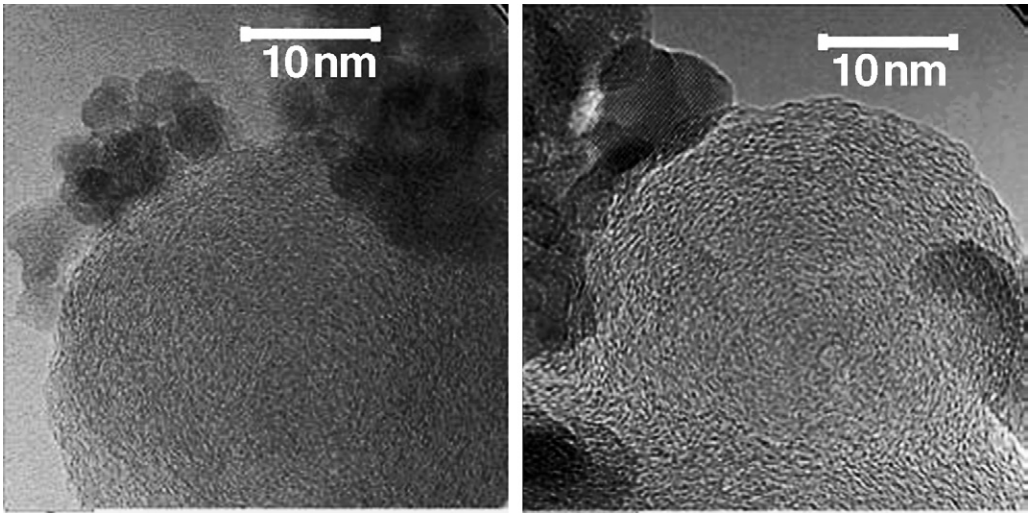

Fig. 12. HRTEM picture of the unreacted mixture of nano-sized Fe_2O_3 and soot (left) and of the corresponding mixture that is obtained after quenching the TPO at a soot conversion of 90% (right).

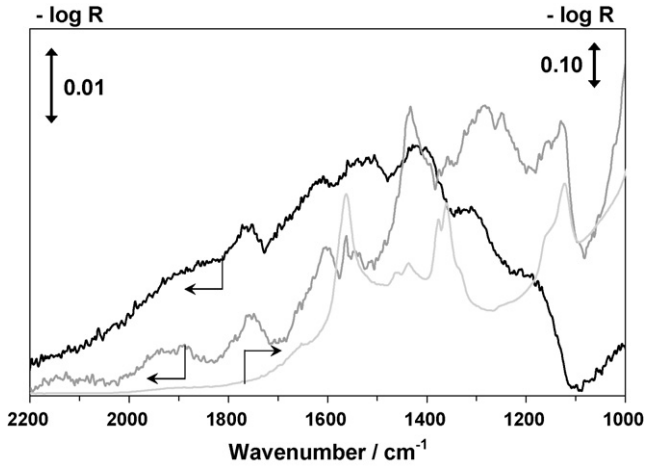

Fig. 13. DRIFT spectrum of pure soot (▬), its mixture with nano-sized Fe_2O_3 (▬) and pure nano-sized Fe_2O (▬); data are recorded at 50 °C under N_2 flow ($n(Fe_2O_3)/n(C) = 2$).

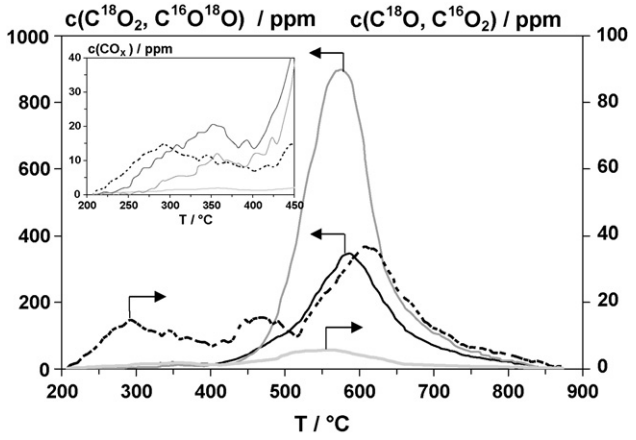

Fig. 14. Concentration of $C^{18}O_2$ (▬), $C^{16}O^{18}O$ (▬), $C^{16}O_2$ (- - -) and $C^{18}O$ (▬) in the catalytic soot/O_2 reaction on Fe_2O_3. The inset shows the respective traces in the beginning of the reaction. Conditions: $m(Fe_2O_3) = 58$ mg (0.38 mmol), m(soot) = 2.2 mg (0.19 mmol C), $c(^{18}O_2) = 0.19$ vol.%, Ar balance, $F = 500$ cm^3/min (STP), $\Delta T/\Delta t = 20$ K/min.

is found in some experiments with catalyst. Thus, from the DRIFTS examinations we derive an absent or at least a very weak interaction between the surface groups of soot and Fe_2O_3 catalyst. In principle, such an interaction might occur between Lewis acid Fe^{3+} sites of the catalyst and free electron pairs of the surface oxygen groups of the soot. This could lead to a decrease in the binding energy of neighbouring (C–C) bonds and thus to an enhancement of the attack of O_2 as proposed by quantum-mechanical calculations from Huang and Yang [43]. However, our DRIFTS data do not support this model of catalytic soot activation. On the other hand the physical contact between soot and catalyst most likely results in van der Waals interaction thus having no impact on the neighbouring (C–C) bond strength and leading to oxygen migration on the soot away from the contact points.

For the examination of the O transfer from the catalyst to soot a TPO of the Fe_2O_3/soot mixture is performed using $^{18}O_2$ labelled oxygen (Fig. 14). With the exception of $C^{16}O$ all possible products are observed, whereas $C^{18}O_2$ represents the major product (232 μmol). However, in the beginning of TPO $C^{16}O_2$ is mainly formed, while $C^{16}O^{18}O$ and then $C^{18}O_2$ are subsequently produced (Fig. 13, inset). For simplicity the traces of $^{18}O_2$, $^{16}O_2$, $^{16}O^{18}O$, $H_2{}^{16}O$ and $H_2{}^{18}O$ detected in TPO and following HTPR are not depicted. Nevertheless, it should be noted that in TPO an excess of oxygen is always present such that reduction of Fe_2O_3 is to be excluded, while in HTPR the catalyst is completely reduced to Fe as indicated by PXRD as well as the mass balance of oxygen (Table 5). Moreover, $^{16}O^{18}O$ and $^{16}O_2$ form above 600 and 700 °C due to exchange of gas-phase $^{18}O_2$ with ^{16}O present in the catalyst. The molar amounts of the reactants and products involved in TPO and HTPR are listed in Table 5 showing that the mass of oxygen is balanced within the analytical limits. Furthermore, these data evidence that in TPO ca. 30% (328 μmol) and thus a substantial abundance of ^{16}O being present in the catalyst is replaced by gas-phase oxygen (^{18}O). However, a significant part of this exchange is related to the adsorption of $^{18}O_2$ producing $^{16}O^{18}O$ (152 μmol) and $^{16}O_2$ (82 μmol). Taking into account these

Table 4
Assignment of the DRIFTS bands of the soot [31,40–42]

Wavenumber (cm^{-1})	Vibration mode	Species
1210	ν(C–O)	Ether, anhydride, phenol, carboxyl
	ν(CH)	Polyaromatic system
1330	ν(C–O)	Lactone
	δ(OH)	Hydroxyl
1420	$\delta(CH_x)$	Bridging CH_2 and terminal CH_3
	δ(OH)	Hydroxyl
1540	ν(C=O)[a]	Carbonyl conjugated to polyaromatic system
1625	ν(C=O)	Chinone, carbonyl
1770	ν(C=O)	Lactone, carboxyl
1850	ν(C=O)	Anhydride
1900	Overtone and combination bands of polyaromatic δ(CH) vibrations	

[a] Superimposed by ν(C=C) vibrations of the polyaromatic system.

Table 5
Molar amounts of oxygen containing reactants and products in TPO of the Fe_2O_3/soot mixture with $^{18}O_2$ and in subsequent HTPR[a]

In		Out	
$n(^{16}O)$ (μmol)	$n(^{18}O)$ (μmol)	$n(^{16}O)$ (μmol)	$n(^{18}O)$ (μmol)
1086 ($Fe_2{}^{16}O_3$)	2993 ($^{18}O_2$)	18 ($C^{16}O_2$)	2220 ($^{18}O_2$)
		55 ($C^{16}O^{18}O$)	55 ($C^{16}O^{18}O$)
		152 ($^{16}O^{18}O$)	232 ($C^{18}O_2$)
		82 ($^{16}O_2$)	1 ($C^{18}O$)
		21 ($H_2{}^{16}O$, TPO)	152 ($^{16}O^{18}O$)
		745 ($H_2{}^{16}O$, HTPR)	33 ($H_2{}^{18}O$, TPO)
			342 ($H_2{}^{18}O$, HTPR)
Sum in: 4079		Sum out: 4108	

[a] Conditions in TPO: $m(Fe_2O_3) = 58$ mg (0.38 mmol), m(soot) = 2.2 mg (0.19 mmol C), $c(^{18}O_2) = 0.19$ vol.%, Ar balance, $F = 500$ cm^3/min (STP), $\Delta T/\Delta t = 20$ K/min; in HTPR same conditions are used with the exception of feed composition (10 vol.% H_2, 90 vol.% Ar).

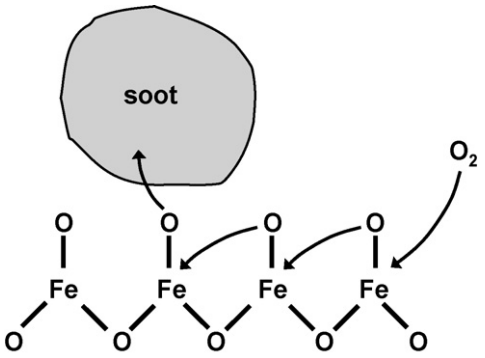

Fig. 15. Mechanistic scheme of the oxygen transfer from the Fe_2O_3 catalyst to soot.

adsorption/desorption processes an amount of 112 μmol remains for the transfer of ^{16}O from Fe_2O_3 to soot. This fraction corresponds to ca. 1 monolayer of surface oxygen as derived from the absolute surface area of the Fe_2O_3 (0.636 m^2) and the diameter of O^{2-} (0.14 nm) [44]. Furthermore, the isotopic TPO indicates continuous oxygen transfer from the catalyst to the soot as $C^{16}O_2$ and $C^{16}O^{18}O$ are permanently formed. Additionally, it is obvious that the transferred ^{16}O is substituted by ^{18}O that become identical to the ^{16}O surface species resulting in the pronounced production of $C^{18}O_2$.

For the mechanism of the oxygen transfer from the Fe_2O_3 to the soot surface we postulate that the transport mainly proceeds at the contact points of both solids. This suggestion is substantiated by our carbothermal and HRTEM studies that indicate contact between soot and catalyst up to high conversion levels and it is in accordance with the postulated mechanism of Mul et al. [27]. Additionally, our isotopic examination clearly shows that only the surface or sub-surface layers of the iron oxide participate in the oxygen transfer, whereas bulk oxygen is not involved. Furthermore, we follow Mul et al. who exclude a substantial spillover of oxygen from the Fe_2O_3 as derived from isotopic studies carried out with different catalysts [27].

Moreover, it is obvious that the Fe sites located at the contact points to the soot are partially reduced during the oxygen transport. In principle, these sites are reoxidised by gas-phase oxygen that is present in excess. However, as the main part of the surface oxygen of the catalyst is involved we suppose that the iron is reoxidised by neighbouring oxygen leading to a kind of cascade of formation and refilling of surface oxygen vacancies. The vacancies produced in a certain distance to the soot contact points are finally refilled by gas-phase oxygen. Additionally, it is generally accepted in the literature [45,46] that O_2 adsorbs dissociatively on Fe_2O_3 with an activation energy that is 0 or very close to 0 kJ/mol [47]. A scheme of our postulated model of oxygen transfer from the Fe_2O_3 catalyst to soot is illustrated in Fig. 15. This mechanism implies that the reaction of soot with oxygen proceeds on the soot surface without direct participation of the catalyst. The role of the catalyst lies in the activation of the soot surface by providing atomic oxygen.

4. Conclusions

Our examinations show that the NO reduction on the Fe_2O_3/soot mixture occurs on the soot surface without being directly affected by the catalyst. Furthermore, O_2 is considered to be crucial for the NO/soot reaction as it produces CC(O) complexes that decompose and lead to the formation of active carbon sites with suitable orientation of the atomic orbitals. Such appropriate surface configuration facilitates the dissociation of NO and formation of N_2. Additionally, NO_2 can accelerate the NO reduction by enhancing the formation of the CC(O) groups, but it is not directly involved in the N_2 formation. The nature of the N species formed on the soot seem to depend on the temperature and/or the presence of the Fe_2O_3 catalyst. Moreover, the role of the catalyst is to transfer atomic oxygen to the soot surface. Our postulated model includes the dissociative adsorption of O_2 and surface migration of O to the contact points of soot and catalyst, whereas no electronic interaction between them is evidenced. At these locations the oxygen is transferred to the soot, whereas the contact points maintain even up to high soot conversion levels. Thus, it is concluded that the catalyst affects the soot oxidation without intermission. Finally, our studies show that only surface and sub-surface oxygen of the Fe_2O_3 catalyst is involved in the oxygen transport.

References

[1] M.V. Twigg, Appl. Catal. B 70 (2007) 2.
[2] P. Balle, H. Bockhorn, B. Geiger, N. Jan, S. Kureti, D. Reichert, T. Schröder, Chem. Eng. Process. 45 (2006) 1065.
[3] F. Kapteijn, A.J.C. Mierop, G. Abbel, J.A. Moulijn, J. Chem. Soc., Chem. Commun. 16 (1984) 1085.
[4] N. Kakuta, S. Sumiya, K. Yoshida, Catal. Lett. 11 (1991) 71.
[5] Y. Teraoka, K. Nakano, S. Kagawa, W.F. Shangguan, Appl. Catal. B 5 (1995) L181.
[6] W.F. Shangguan, Y. Teraoka, S. Kagawa, Appl. Catal. B 8 (1996) 217.
[7] Y. Teraoka, K. Nakano, W.F. Shangguan, S. Kagawa, Catal. Today 27 (1996) 107.
[8] W.F. Shangguan, Y. Teraoka, S. Kagawa, Appl. Catal. B 16 (1998) 149.
[9] Y. Teraoka, K. Kanada, S. Kagawa, Appl. Catal. B 34 (2001) 73.
[10] K. Matsuoka, H. Orikasa, Y. Itoh, P. Chambrion, A. Tomita, Appl. Catal. B 26 (2000) 89.
[11] S. Xiao, K. Ma, X. Tang, H. Shaw, R. Pfeffer, J.G. Stevens, Appl. Catal. B 32 (2001) 107.
[12] W. Weisweiler, K. Hizbullah, S. Kureti, Chem. Eng. Technol. 25 (2002) 140.
[13] S. Kureti, K. Hizbullah, W. Weisweiler, Appl. Catal. B 3 (2003) 281.
[14] S. Kureti, K. Hizbullah, W. Weisweiler, Chem. Eng. Technol. 26 (2003) 1003.
[15] N. Nejar, J.M. Garcia-Cortes, C.S.M. de Lecea, M.J. Illan-Gomez, Catal. Commun. 6 (2005) 263.
[16] D. Fino, N. Russo, G. Saracco, V. Specchia, J. Catal. 242 (2006) 38.
[17] W.F. Shangguan, Y. Teraoka, S. Kagawa, Appl. Catal. B 12 (1997) 237.
[18] Y. Teraoka, W.F. Shangguan, S. Kagawa, Res. Chem. Intermed. 2 (2000) 201.
[19] H. Yamashita, A. Tomita, A. Yamada, T. Kyotani, L.R. Radovic, Energy Fuels 7 (1993) 85.
[20] J. Yang, G. Mestl, D. Herein, R. Schlögel, J. Find, Carbon 38 (2000) 715.
[21] J.E. Johnsson, Fuel 73 (1994) 1398.
[22] H. Teng, E.M. Suuberg, J.M. Calo, Energy Fuels 6 (1992) 398.
[23] J. Yang, G. Mestl, D. Herein, R. Schlögl, J. Find, Carbon 38 (2000) 729.

[24] T. Suzuki, T. Kyotani, A. Tomita, Ind. Eng. Chem. Res. 33 (1994) 2840.
[25] P. Chambrion, T. Suzuki, Z.H. Zhang, T. Kyotani, A. Tomita, Energy Fuels 11 (1997) 681.
[26] T. Kyotani, A. Tomita, J. Phys. Chem. B 103 (1999) 3434.
[27] G. Mul, F. Kapteijn, C. Doornkamp, J.A. Moulijn, J. Catal. 170 (1998) 258.
[28] G. Mul, J.P.A. Neeft, F. Kapteijn, J.A. Moulijn, Carbon 36 (1998) 1269.
[29] H. Dörr, H. Bockhorn, R. Suntz, in: Proceedings of the 8th ETH Conference on Combustion Generated Particles, Zürich, 2004.
[30] B.A.A.L. van Setten, J.M. Schouten, M. Makkee, J.A. Moulijn, Appl. Catal. B 28 (2000) 253.
[31] A. Setiabudi, M. Makkee, J.A. Moulijn, Appl. Catal. B 50 (2004) 185.
[32] P. Ehrburger, J.F. Brilhac, Y. Drouillot, V. Logie, P. Gilot, SAE Paper 2002-01-1683.
[33] C. Li, T.C. Brown, Carbon 39 (2001) 725.
[34] D.R. Lide (Ed.), Handbook of Chemistry and Physics, 74th edition, CRC Press, Boca Raton, 1994.
[35] Q. Zhu, S.L. Money, A.E. Russel, K.M. Thomas, Langmuir 13 (1997) 2149.
[36] J.M. Carlsson, M. Scheffler, Phys. Rev. Lett. 96 (2007) 046806.
[37] L.S. Darken, R.W. Gurry, J. Am. Chem. Soc. 68 (1946) 798.
[38] E.E. Unmuth, L.H. Schwarz, J.B. Butt, J. Catal. 61 (1980) 242.
[39] A. Bessier, J. Bessieres, P. Becker, J.J. Heizmann, Mém. Sci. Rev. Mét. 76 (1979) 397.
[40] M.A. Akhter, A.R. Chughtai, D.M. Smith, Appl. Spectrosc. 39 (1985) 143.
[41] M.S. Akhter, A.R. Chughtai, D.M. Smith, J. Phys. Chem. 88 (1984) 5334.
[42] W.W. Simmons, The Sadtler Handbook of Infrared Spectra, Sadtler Research Laboratories, Philadelphia, 1978.
[43] H.Y. Huang, R.T. Yang, J. Catal. 185 (1999) 286.
[44] K. Sakatam, F. Ueda, M. Misono, Y. Yoneda, Bull. Chem. Soc. Jpn. 53 (1980) 324.
[45] H. Randall, R. Doepper, A. Renken, Ind. Eng. Chem. Res. 36 (1997) 2996.
[46] G. Bergeret, P. Gallezot, Handbook of Heterogeneous Catalysis, vol. 2, Wiley, New York, 1997.
[47] D. Reichert, P. Balle, T. Finke, B. Geiger, S. Kureti, in preparation.